International Journal of Greenhouse Gas Control 86 (2019) 191–200

Contents lists available at ScienceDirect

International Journal of Greenhouse Gas Control

journal homepage: www.elsevier.com/locate/ijggc

# Field test of a pre-pilot scale hollow fiber facilitated transport membrane for $CO_2$ capture

Zhongde Dai[a], Santinelli Fabio[b], Nardelli Giuseppe Marino[b], Costi Riccardo[b], Liyuan Deng[a,*]

[a] Department of Chemical Engineering, Norwegian University of Science and Technology, Trondheim, 7491, Norway
[b] Colacem S.p.A., Via della Vittorina n. 60, 06024, Gubbio, PG, Italy

ARTICLE INFO

*Keywords:*
$CO_2$capture
Field test
Flue gas
Hollow fiber membrane
Facilitated transport

ABSTRACT

In this work, a pre-pilot scale hollow fiber membrane module with a PVA/ProK hybrid membrane containing up to 40 wt% amino acid salt was fabricated and tested infield for $CO_2$ capture. The petroleum coke-fired flue gas generated from the rotary kiln provided with a 5-stage cyclone pre-heater tower for the production of grey clinker in the Colacem cement plant in Gubbio (PG), Italy, was used as feed gas after a simple filtration to remove the suspended particulate matter without further pretreatment. The temperature for the membrane test was ranging from 80 to 115 °C. The effects of various parameters including operation temperature, pressure, sweep gas flow rate, vacuum grade, and the impurities in the feed were systematically investigated. Under optimized condition, $CO_2$ content of 50% in the permeate and $CO_2$ permeate flux of ~$5 \times 10^{-3}$ $cm^3$(STP) $cm^{-2}$ $s^{-1}$ were documented, which is comparable with other facilitated transport membranes. The presence of impurities in the feed stream showed a negligible effect on the $CO_2$ separation performance. Long-term stability was also studied through a test for a duration of 1 week at 90 °C.

## 1. Introduction

It is commonly accepted that $CO_2$ capture is an effective way to combat climate change, as carbon capture and sequestration (CCS) could mitigate $CO_2$ emission into the atmosphere with the possibility of continuously using fossil fuels without causing significant $CO_2$ emissions (Benson and Orr, 2008; Li et al., 2018). Among the $CO_2$ emission sources (e.g., power production, transportation and other industry processes), large $CO_2$ point sources such as fossil fuel power plants and industrial plants, particularly the production units of iron, steel, cement and chemicals, and natural gas plants are more likely to be used for $CO_2$ capture with relatively lower cost (Bains et al., 2017). Up to now, numerous technologies have been proposed for $CO_2$ capture, including chemical absorption/adsorption, physical absorption/adsorption, chemical looping, and membrane separation. Among these options, membranes clearly represent one of the emerging technologies to be used for $CO_2$ capture (Rafiq et al., 2016).

Membrane technology is a cost-effective and energy-efficient separation process for $CO_2$ removal due to low capital cost, low energy penalty, and operational simplicity relative to other competitive technologies (Nunes and Peinemann, 2006). In addition, membrane processes could adapt almost instantaneously to changing process conditions. Hence numerous investigations dealt with the development of membrane materials for the separation of $CO_2$ from nitrogen or hydrogen have been published (Baker and Low, 2014; Galizia et al., 2017). However, despite of a large number of membrane materials developed in lab scale as self-standing membranes, only a few can be fabricated into thin-film-composite membranes with feasible $CO_2$ permeance, and even fewer were used to produce membrane modules that could be employed for a pilot-scale test.

Up to now, there are only handful examples of pre-pilot or pilot scale field tests applying membrane for $CO_2$ capture from flue gas of different relevant emission sources (e.g., power plant and cement plant, as shown in Table 1). Polaris™ membrane is one of the representative membranes for $CO_2$ capture developed by Membrane Technology & Research, Inc. (White et al., 2015). It has been applied in several pilot plant tests, including the separation of $CO_2$ from flue gas and hydrogen (Lin et al., 2014; Merkel et al., 2010; White et al., 2015). A $CO_2$ permeance values in the range of 1000–2000 GPU (50 psig, 23 °C) and $CO_2/N_2$ selectivity in the range of 50–60 were obtained for this membrane. Another example is the Polyactive™ membrane developed by the Institute of Polymer Research of Helmholtz-Zentrum Geesthacht (HZG), which has been applied in $CO_2$ capture from a power plant flue gas for the cultivation of algae (Brinkmann et al., 2015; Pohlmann et al., 2016; Wolff et al., 2015). The Polyactive™ membrane presents $CO_2$ permeance of ~740 GPU (single gas permeation data obtained at 30 °C with a feed

* Corresponding author.
*E-mail address:* deng@nt.ntnu.no (L. Deng).

https://doi.org/10.1016/j.ijggc.2019.04.027
Received 19 February 2019; Received in revised form 15 April 2019; Accepted 30 April 2019

**Table 1**
Summary of membrane pilot scale $CO_2$ capture test.

| Membrane materials | Membrane type | Feed Pressure | Temp (°C) | Permeate pressure | $CO_2$ permeance (GPU) | $CO_2$ flux | Selectivity/purity in permeate | Ref |
|---|---|---|---|---|---|---|---|---|
| Polaris | SW | 1.37–2.06 bar | 68–74 | vacuum + sweep gas (air) | 1000–2000 (50 psig, 23 °C) | – | 50–60 | (White et al., 2015)[#] |
| Polaris | SW | 13.4 bar | 20 | – | 100–300 (20 °C) | – | 20–50 for $CO_2/N_2$, 6–10 for $CO_2/H_2$ | (Lin et al., 2014)[#] |
| PES | HF | 6˜8 bar | – | – | 60 | – | 40 | (Choi et al., 2013)[#] |
| Polyactive | PF | 1.132 bar | 25–35 | 100 mbar | 100–1200 | – | 43–60 | (Pohlmann et al., 2016)[#] |
| Polyactive | PF | 1 bar | RT | 180 mbar | – | – | 40–50% $CO_2$ in permeate side | (Wolff et al., 2015) |
| Polyactive | PF | 4 bar | 25 | 0.11–0.54 bar | – | – | 70–80% in permeate side | (Brinkmann et al., 2015) |
| Polyactive | PF | 7–9 bar | 16–25 | 1 bar | – | – | 70–80% $CO_2$in permeate side | (Brinkmann et al., 2015)[#] |
| Polyactive | PF | 10–20 bar | 22–24 | 1.35 bar | – | ˜762 NLm$^{-2}$h$^{-1}$ | 56–67% $CO_2$ in permeate side | (Brinkmann et al., 2015) |
| Prism (polysulfone) | HF | 1.32 bar | RT | 0.11 bar | 400–500 | ˜142 NLm$^{-2}$h$^{-1}$ | 3–6 | (Scholes et al., 2015) |
| NF3838/30 F(polyamide) | SW | 1.32 bar | RT | 0.11 bar | 10–30 | ˜11 NLm$^{-2}$h$^{-1}$ | 5–10 | |
| PVAm (FSC) | HF | 2.5 bar | 35 | 250 mbar | 740 | ˜500 NLm$^{-2}$h$^{-1}$ | 135 | (He et al., 2015) |
| PVAm (FSC) | PF | 1 atm | 45 | 130 mBar | 180–220 | ˜80 NLm$^{-2}$h$^{-1}$ | 80–300, ˜50% $CO_2$ in permeate side | (Sandru et al., 2013) |
| PVAm (FSC) | HF | 1–6 bar | 23–45 | 0.1–0.4 bar | – | ˜20 NLm$^{-2}$h$^{-1}$ | ˜65% $CO_2$ in permeate side | (He et al., 2017) |
| FTM[(1)] | SW | 4 atm | 57–87 | 0.3 atm | 1450 | – | ˜185, $CO_2$ purity in permeate up to 94.5 % | (Han et al., 2019) |
| FTM[(2)] | SW | 1.5 psig | 57 | sweep, 1 psig | 800 | ˜160 NLm$^{-2}$h$^{-1}$ | 140 | (Salim et al., 2018) |
| FTM[(3)] | HF | 2 bar | RT | sweep, 1 psig | 790 | – | ˜40 | (Dai et al., 2019)[##] |

FSC—fixed site carrier, FTM—facilitated transport membranes, SW—spiral-wound, HF—hollow fiber, PF—plate and frame. PES- Poly(ether sulfone), PVAm- polyvinylamine. FTM[(1)] was flat sheet membranes fabricated using poly(N-vinylformamide-co-vinylamine) (PNVF-co-VAm) as fixed-site carrier and 2-(1-piperazinyl)ethylamine sarcosinate (PZEA-Sar) as mobile carrier. FTM[(2)] was flat sheet membrane fabricated using Piperazine, glycine, and PVAm. FTM[(3)] was hollow fiber membranes fabricated from PVA and amino acid salts. GPU is used as the gas permeation unit. 1 GPU = $10^{-6}$ cm$^3$ (STP) cm$^{-2}$ s$^{-1}$ (cm Hg)$^{-1}$
[#] Water vapor needs to be removed. [##]Gas permeation results obtained from lab scale tests.

pressure of 1 bar) with a $CO_2/N_2$ selectivity of ˜40 (Yave et al., 2010). Both the Polaris™ membrane and Polyactive™ membranes in these works are in the form of spiral wound membrane modules. In another study carried out as part of the Cooperative Research Centre for Greenhouse Gas Technologies (CO2CRC) H3 project (Qader et al., 2017), two membrane modules were used for post-combustion $CO_2$ capture in pilot scale. These two modules are the Air Products PRISM module filled with asymmetric glassy polymeric hollow fibers, and the commercial thin-film-composite (TFC) polyamide membrane (Dow NF3838/30FF) in a spiral wound module designed for nanofiltration applications (Scholes et al., 2015).

Due to the low $CO_2$ partial pressure and presence of water vapor in flue gases, post-combustion $CO_2$ capture can be challenging for membranes based on solution-diffusion separation mechanisms. The competitive sorption between water and permeating gases may lead to a serious reduction in both $CO_2$ permeance and $CO_2/N_2$ selectivity (Scholes et al., 2015). Furthermore, water molecules in the feed stream could also lead to serious plasticization for polymeric membranes, which may permanently alter the membrane structure, leading to a dramatic decrease in gas permeance and selectivity; the initial performance does not always return once the membrane is dried (Scholes et al., 2009). Therefore, sometimes an extra step is needed to remove the water vapor, which increases the complexity of the process and operation cost.

An alternative approach is facilitated transport membranes, which have shown the potential to achieve permeances and selectivities substantially higher than conventional polymeric membranes due to the reversible reaction mechanism of $CO_2$ with the carrier agent in the presence of water (Ward and Robb, 1967; Way et al., 1987). PVAm (polyvinylamine)-based fixed site carrier (FSC) facilitated transport membrane is one of the representative facilitated transport membranes, and has been intensively studied at NTNU (Norwegian University of Science and technology) in Norway (Deng and Hägg, 2010, 2014, 2015; Deng et al., 2009; Kim et al., 2013). Due to the excellent separation performance in the lab scale (Kim et al., 2013), the PVAm-based FSC membranes were developed into pilot scale plate-and-frame module and tested in-field for $CO_2$ capture from coal-fired power plants flue gas in Portugal, 2013 (Sandru et al., 2013). The membrane was later fabricated as pilot scale hollow fiber membrane module and tested in a cement plant in Brevik, Norway, in 2015 (Hägg et al., 2017). Ho and coworkers have also fabricated Poly(allylamine) (PAA) based facilitated transport membrane into pilot scale spiral-wound membrane modules, and tested at the National Carbon Capture Center in Wilsonville, Alabama, USA (Salim et al., 2018). The performances of the facilitated transport membranes modules are summarized in Table 1 for comparison.

In the above mentioned facilitated transport membranes, the facilitated transport effect mainly comes from the reverse reaction between the amino groups from the polymer chain (e.g., PVAm or PAA) and $CO_2$ gas molecules. Recently, due to the fast reaction kinetics and high $CO_2$ absorption capacity, amino acid salts were used as mobile carriers in facilitated transport membranes. It has been reported that adding amino acid salts into different polymeric matrix (e.g., chitosan, SPEEK (sulfonated poly(ether ether ketone), PVAm, and PVA) (El-Azzami and Grulke, 2009; Qin et al., 2016; Tong and Ho, 2017; Dai et al., 2019) could effectively improve the $CO_2$ permeance/permeability.

This work focuses on the up-scaling and fabrication of a PVA/amino acid salt hybrid hollow fiber membrane, and the field test of the developed pre-pilot scale membrane module in a cement plant. Various effects of operating parameters on the separation performance and the material durability were investigated. The PVA/amino acid salt hybrid membrane was selected for the field test based on a prior study (Dai et al., 2019), where four amino acid salts were embedded into polyvinyl alcohol (PVA) matrix and the optimized membrane showed the $CO_2$ permeance of up to ˜800 GPU with a $CO_2/N_2$ selectivity of ˜40. The

membrane presented a stable performance at elevated temperatures throughout 2 weeks (shown in Table 1). In the current work, the field tests were carried out in a cement plant with the petroleum coke-fired flue gas coming from a rotary kiln with a 5-stage pre-heater as the feed gas. The influences of the different process conditions, including the operation temperature (80–115 °C), feed gas pressure (1.5–2.0 bar), sweep gas flow rate (0.4–1.5 L/min), vacuum grade (0.2–0.8 bar, or the residual pressure ranging from 0.8 to 0.2 bar), and water content in the feed stream, were assessed and analyzed. In addition, the stability of the membrane was studied through a continuous permeation test at 90 °C for one week.

## 2. Experimental

### 2.1. Materials

Poly(vinyl alcohol) (PVA, Mn 7.9k–12k, 89% hydrolyzed), L-proline, and potassium hydroxide (KOH) were ordered from Sigma, Germany. All chemicals were used as received without further purification. Poly (*p*-phenylene oxide) (PPO) hollow fiber membrane was kindly supplied by Parker, Norway. The surface of the PPO supports were gently washed with DI water and dried at ambient condition for at least 6 h before the selective layer was coated.

### 2.2. Membrane preparation

The membrane used in the field test was a thin film composite hollow fiber membrane with a selective layer made of the PVA/amino acid salt hybrid (Dai et al., 2019). The support substrate was a PPO hollow fiber membrane. The selective layer has a thickness of app. 500 nm. A brief description of the membrane preparation steps is given as follows. First, PVA solution (4 wt%) was prepared by dissolving PVA in water at 80 °C for 4 h under reflux, and the amino acid salt (ProK) was synthesized by mixing the stoichiometric amount of proline with KOH in DI water (10 wt%). Second, the desired amounts of the ProK and PVA solution were mixed to make a solution with ProK content of 40 wt%. Then the total solid (PVA + ProK) concentration in the coating solution was diluted to 0.5 wt% in water. The PVA/amino acid salt solution was filtrated using the 0.65 PTFE filter membrane prior to each membrane coating process. The amino acid salts content ($\omega_{ProK}$, wt%) in each hybrid membrane was calculated from Eq. (1):

$$\omega_{ProK} = \frac{w_{ProK}}{w_{ProK} + w_{PVA}} \times 100 \quad (1)$$

where $w_{ProK}$ and $w_{PVA}$ are the weights of amino acid salt and PVA, respectively. Afterward, dip-coating was employed to fabricate the PVA/ProK selective layer onto the PPO substrate. The soaking time was 10 s. The hollow fiber was prepared manually, so the withdrawn rate was not quantitatively controlled; it was approximately 2–3 s. Further details on the membrane fabrication can be found in our prior study (Dai et al., 2019). In the current work, the membrane fabricated were marked as PVA/ProK-40.

### 2.3. Membrane module fabrication

The membrane modules employed in this study were hollow fiber modules. The pre-pilot scale hollow fiber membrane module was fabricated based on the procedure shown in Scheme 1.

First, the coated HF membranes were put in a 1/2 in. Swagelok™ metal tube with an extra rubbery tube (diameter of 8 mm) set on one end of the tube. It should be aware that the end of the HF membrane must be out of the rubbery tube to avoid the glue from penetrating inside and blocking the membranes. A small amount of fast curing glue was then injected into the rubber tube, set still for curing for ~3 h. Next, a second glue with much lower viscosity was injected into the rubber tube. The low viscous glue was employed to ensure that the glue could go through and fill the voids between the hollow fibers, thus to reduce the possibility of leaking. After the second glue being cured for 12 h, the rubbery tube was removed and the extra part of the glue was cut off using a knife. Finally, another end of the module was prepared by repeating the above procedure.

Fig. 1 shows the optical image of the hollow fiber membrane modules used in the lab scale test at NTNU and the pre-pilot scale test membrane modules used in the cement plant at Colacem. In a lab scale membrane module, only 10 hollow fibers were mounted inside the module, while in a pre-pilot scale membrane module, 70 fibers with doubled length (20 cms compared to 10 cms) were installed.

Detailed information about the two membrane modules is listed in Table 2.

### 2.4. Membrane characterization

In this work scanning electron microscope (SEM, TM3030 tabletop microscope, Hitachi High Technologies America, Inc.) was used to investigate the morphology of the hollow membranes. All samples were sputter coated with conductive gold.

Fourier-transform infrared spectroscopy (FTIR) spectra of the PVA/Prok-40 HF membranes were measured using a Nicolet iS-50 FTIR spectrometer equipped with a Specac ATR unit (Golden Gate high performance single reflection monolithic diamond ATR) within the range between 4000 and 650 $cm^{-1}$. The result was an average of 16 scans.

Thermogravimetric analysis (TGA, TG 209F1 Libra) was used to determine the amount or rate of weight changes as a function of temperature over time in a controlled atmosphere ($N_2$). About 10 mg of the sample heated from R.T. to 800 °C with a heating rate of 10 °C/min.

### 2.5. In-field gas permeation test and flue gas conditions

The test was carried out using flue gas from the emission stack (height: 105 m) placed close to the 5-stage cyclone pre-heater of the grey clinker production line at the Colacem Cement Plant located in Gubbio (PG) Italy (as shown in Fig. 2).

The sampling point was located 30 m below the top of the stack. A hole was made on the sidewall of the chimney and the vacuum pump was used to suck the flue gas from the chimney to the membrane module (as shown in Fig. 2). A 2 μm ceramic filter, part of the gas sample probe (M&C Model SP180 H), was used to remove the suspended particulate matter in the flue gas. The temperature of the flue gas from the stack, during the plant tests, was about 115 °C. The composition of the dry flue gas during the plant tests is summarized in Table 3. The flue gas contains 9%–11% of water vapor in addition to the mixture of gases.

The flow chart of the in-field membrane permeation test is shown in Fig. 3(A). Except for the removal of suspended particulate matter from the flue gas by the filter, no further pretreatment was carried out for the feed gas. All the gas transport pipes were covered by electric heating tubing bundle to control the desired temperature for the test mainly to avoid humidity condensation. One needle valve was placed at the retentate side to control the feed pressure. The gas composition of the feed gas was measured by the Multicomponent Analysis System ACF-NT of ABB S.p.A., while that of the retentate and permeate streams was measured by the HORIBA PG 350 SRM and with TESTO Model 350XL-350S gas analyzers. The flow rates of the three streams were measured by TSI Model 4143 and confirmed by some floating element flow meters selected in accordance with the flow rate to be measured. If not specified, all the tests were carried out without vacuum or sweep gas. In the case that sweep gas was used, the composition of the IP grade gas was: 20.93% Oxygen and 79.07% Nitrogen.

Tests were also carried out to investigate the effect of the water content in the feed. Simulated flue gas from a gas cylinder with $CO_2$/$O_2$/$N_2$ mixture (12.6/14/73.4% vol) was used as the feed gas, where

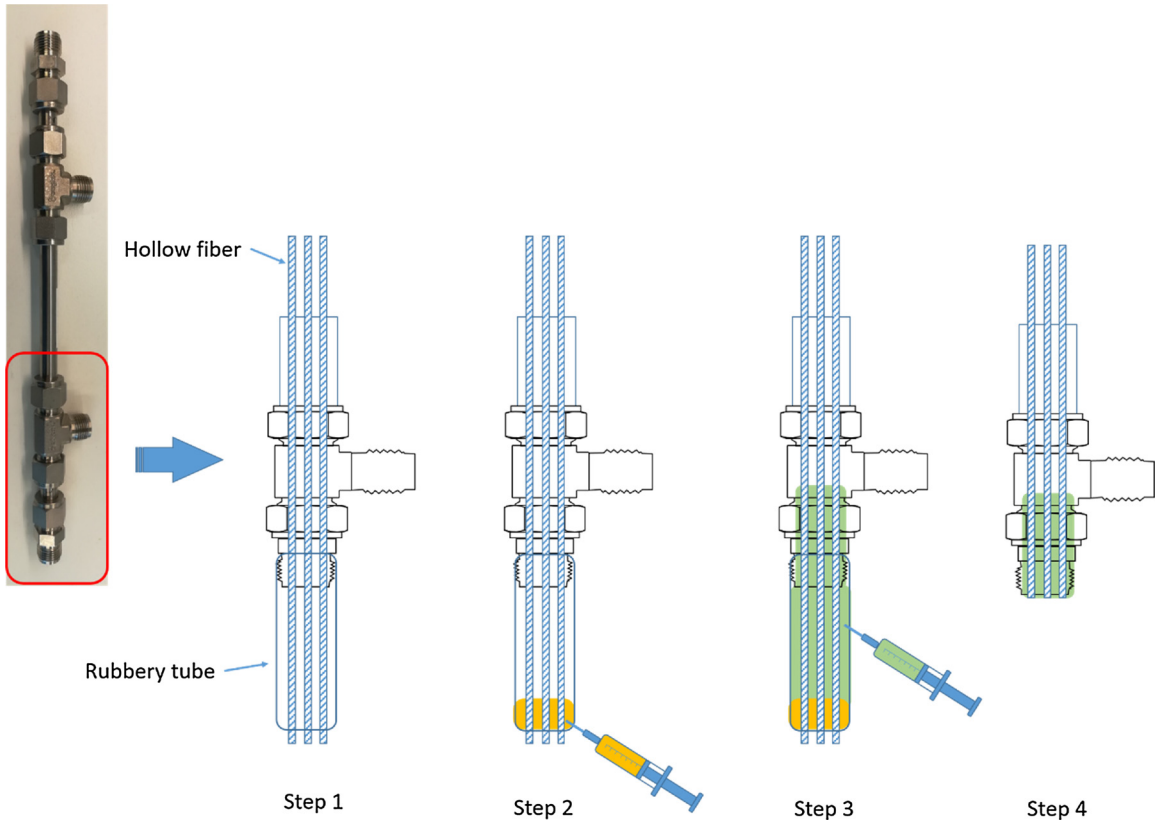


**Scheme 1.** Hollow fiber membrane module preparation.

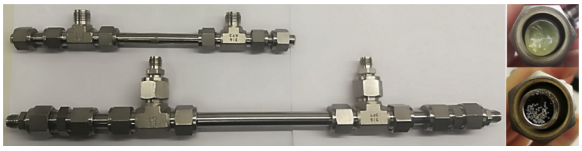

**Fig. 1.** Comparison of the lab scale membrane module and pre-polite scale membrane modules.

**Table 2**
Detailed dimension about lab scale and pre-polite scale membrane modules.

| | Lab scale | Pre-pilot scale |
|---|---|---|
| Fiber number (-) | 10 | 70 |
| Effective length (cm) | 10 | 20 |
| Effective membrane area ($cm^2$) | ~16 | ~200 |
| Coating method | Hand dip-coating | Half-automatic dip-coating |
| Host material size | 3/8 in. | 1/2 in. |

water was added into the feed stream by a water evaporator. The temperature and feed flow rate in the water evaporator was controlled to adjust the humidity of the feed gas, as shown in Fig. 3(B).

The $CO_2$ flux was calculated based on the flow rate and the $CO_2$ composition in the permeate stream as shown in Eq. (2).

$$Q_{CO_2} = \frac{N_{per} \times y_{CO_2,per}}{A} \quad (2)$$

Where the $Q_{CO_2}$ is the $CO_2$ flux through the membrane ($cm^3$(STP)/$cm^2$s), $N_{per}$ is the flow of the permeate stream (L/min), $A$ is the effective membrane area ($cm^2$), and $y_{CO_2,per}$ is the $CO_2$ concentration in the permeate side (%). The $CO_2$ flux was also double checked by calculating the mass balance of the feed side and the retentate side.

## 3. Results and discussion

### 3.1. Characterization of the hollow fiber membrane

Different techniques were used to characterize the fabricated PVA/ProK-40 membranes, as shown in Fig. 4.

From the SEM images shown in Fig. 4 (A) a layer with a thickness of around 500 nm has been evenly coated onto the hollow fiber PPO substrate. In Fig. 4 (B), the FTIR spectrum of pure PVA and PVA with 40 wt% ProK. Fig. 4(C) shows the TGA curve of PVA and PVA/ProK-40. The presence of the ProK salt slightly reduces the thermal stability of the membranes, but it still fulfills the requirement of common post-combustion $CO_2$ capture processes. Gas permeation properties of the membrane were also investigated at lab scale under room temperature condition, as shown in Table 4.

### 3.2. Gas separation performances in real stream flue gas

#### 3.2.1. Effect of operation temperature and feed pressure

It is well-known that the operating temperature has significant impacts on the gas separation performance of membranes. In the case of membranes based on the solution-diffusion model, increasing temperature usually leads to the increase of diffusivity but decrease in solubility. Concerning facilitated transport, however, there may exist an optimal temperature based on the kinetics of the reversible reaction involved in the $CO_2$-carrier interaction (El-Azzami and Grulke, 2009; Xing and Ho, 2011).

In the current study, the effect of temperature on separation performances was investigated in the range of 60–115 °C (Fig. 5). When the temperature was lower than 80 °C, the water vapor in the feed gas severely condensed in the tube. No reliable permeation data were obtained at this temperature range. In the range of 80 to 100 °C, $CO_2$ flux firstly slightly increased with increasing temperature, but then dropped

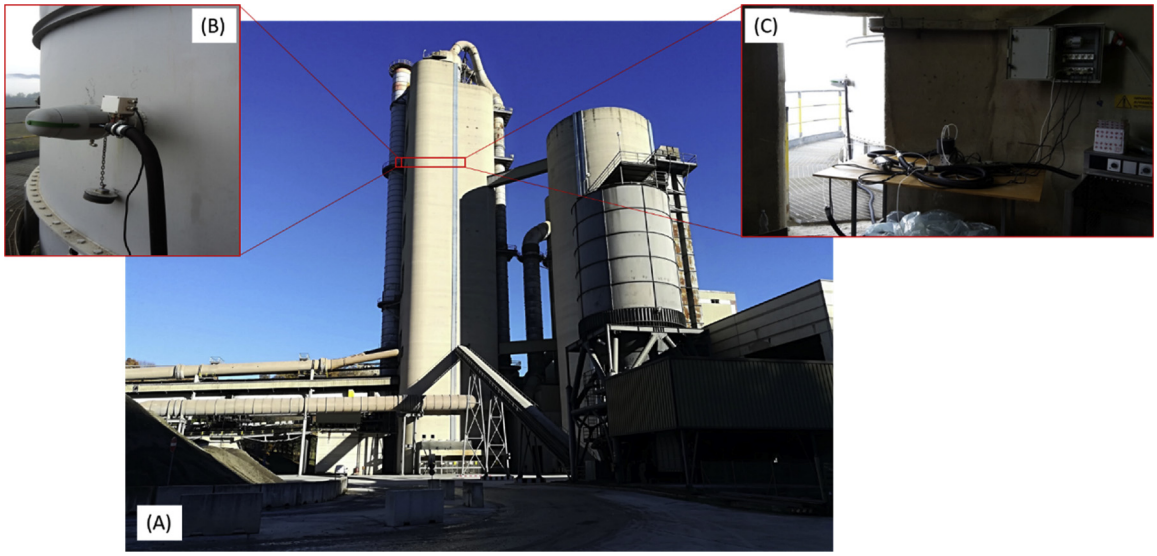


**Fig. 2.** Field test point in the cement plant, (A) grey clinker rotary kiln with its 5-stage cyclone pre-heating tower and the gas emission stack in Colacem S.p.A. cement plant located in Gubbio (PG), Italy, (B) Sampling point of the flue gas from the emission stack, (C) Permeation test rig located in the preheating tower.

**Table 3**
Composition of the flue gas from the grey clinker production line.

| Components | Concentration in the dry flue gas |
|---|---|
| $CO_2$ (%v/v) | 11.5–14.0 |
| $O_2$ (%v/v) | 12.5–14.5 |
| $N_2$ (%v/v) | 72–76 |
| CO (ppmv) | 160–200 |
| NOx (ppmv) | 135–150 |
| SOx (ppmv) | 0–1 |
| $NH_3$ (ppmv) | 15–50 |
| HCl (ppmv) | 0.5–1 |
| Suspended Particulate Matter (mg/$Nm^3$) | 2–5 |

again at 100 °C. Temperature affects the facilitated transport in many different ways. First of all, as temperature increases, gas diffusion increases and the rate of reaction between $CO_2$ and the carrier increases, resulting in an overall increase in $CO_2$diffusion. However, with increasing temperature, the sorption of $CO_2$ in the membrane decreases. In addition, increasing temperature causes a decrement of water retention in the membrane (owing to the lower relative humidity at higher temperature), which in turn hinders the reaction and diffusion. These effects compete with each other and their influences vary significantly, depending on the materials and the interactions involved. Therefore, different membrane materials normally exhibit quite different optimized temperature with respect to $CO_2$ separation performance. For instance, the optimized operation temperature for PVA/PAA gel membrane with 2,3-diaminopropionic acid (DAPA) as mobile carrier is 125 °C (Yegani et al., 2007), while for sulfonated polybenzimidazole copolymer based facilitated transport membranes, the optimized operation temperature is 100 °C (Bai and Ho, 2009). It is worth mentioning that the optimized operation temperature is also affected by the operation pressure (Bai and Ho, 2011), which changes from 110 °C to 106 °C when the operation pressure increases from 2 bar to 15 bar for crosslinked PVA/amine membranes. In the current study, it was found that a further increase in temperature to 115 °C resulted in an extremely low permeate flow (undetectable). The possible explanation can be that under high temperature conditions, the polymeric selective layer and support lose rigidity and become susceptible to compaction.

In this study, the membrane module was tested infield with the feed pressure varying in the range of 1.5–2 bar and no sweep gas or vacuum were used on the permeate side. The $CO_2$ flux across the membrane as a function of feed pressure is shown in Fig. 6. As it can be seen, increasing feed pressure increases the overall $CO_2$ flux, but the value is lower than the ideal case of a polymeric membrane following the solution-diffusion mechanism (presented as a red line in Fig. 6), which is probably due to the typical carrier-saturation phenomenon in facilitated transport membranes (Way and Noble, 1992). For example, Ho and co-workers reported a notable reduction of $CO_2$ permeability from ~3000 Barrer to ~300 Barrer with a feed pressure increment from 2 bar to 28 bar (Ansaloni et al., 2015), while both $CO_2/N_2$ selectivity and $CO_2/H_2$ selectivity also decreased.

Although the $CO_2$ flux increases with increasing feed pressure, it should be aware that an optimal feed pressure should be determined by considering the trade-off between the energy consumption and the increased flux, or the consequently reduced cost due to the decreased membrane area.

### 3.2.2. *Effect of sweep gas flow rate*

In order to investigate the effects of sweep gas on the overall gas separation performances, air was used as sweep gas in the field test. As shown in Fig. 7, using air with a flow rate of 0.4 L/min as sweep gas dramatically increased the $CO_2$ flux across the membrane from $1.69 \times 10^{-3}$ $cm^3$(STP) $cm^{-2}$ $s^{-1}$ to $3.32 \times 10^{-3}$ $cm^3$(STP) $cm^{-2}$ $s^{-1}$. It is well accepted that due to concentration polarization, both $CO_2$ permeance and $CO_2/N_2$ selectivity obtained at pilot scale usually are lower than the values obtained in the lab. Using sweep flow gas could significantly increase the driving force across the membrane and reduce the concentration polarization effect, thus resulted in a much higher $CO_2$ flux. For instance, the $CO_2$ concentration in the permeate flow reduced from ~48% to 10.6% when 0.4 L/min air was used as the sweep gas. The reduced $CO_2$ concentration in the permeate flow resulted in much higher driving force and thus a higher $CO_2$ flux. Further increasing the sweep flow only led to a moderate enhancement in $CO_2$ flux. For instance, using 0.4 L/min of sweep gas resulted in a big reduction in the $CO_2$ concentration to 10.6%, while increasing the sweep flow rate to 1 L/min and 1.5 L/min resulted in the decrease of the $CO_2$ concentration in the permeate stream to 5.0% and 3.0%, respectively.

In addition, the relative humidity of the air purged into the membrane module is much lower than that of the feed gas in the feed side; thus the relatively dry sweep flow may cause a reduction in the water content in the membrane, which may have hindered the $CO_2$ transport through the membrane.

When a sweep gas was applied in the field test, the $CO_2$ partial

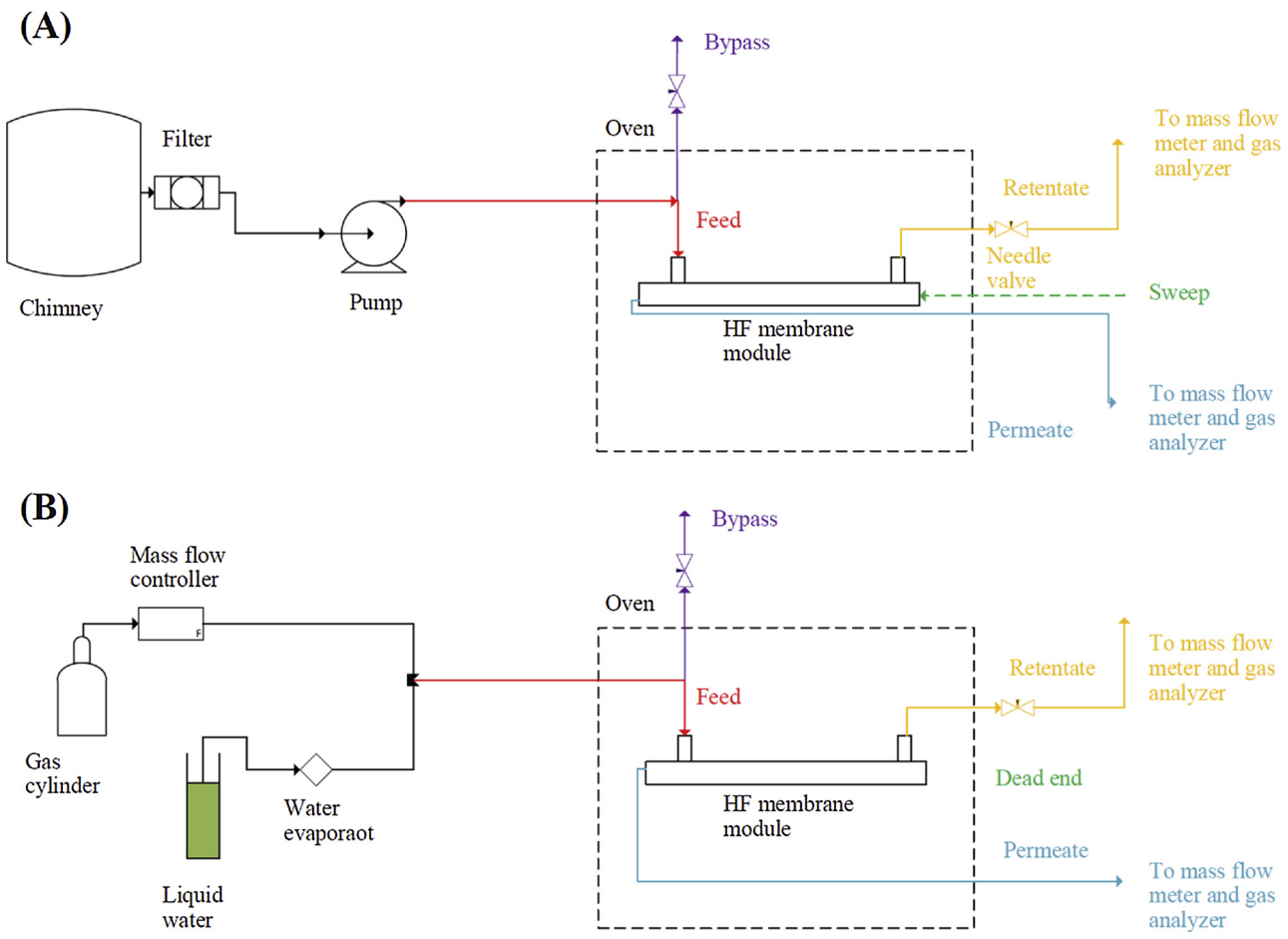


**Fig. 3.** Process flow charts for the gas permeation test. (A) Flue gas is used as the feed gas in the permeation test. A membrane pump (KNF Model N036-ST-11-E) is used to suck the flue gas from the chimney. The basic operation conditions are feed flow 3.5 L/min; feed pressure 1.5 bar; temperature 90 °C; no sweep gas. (B) Synthetic flue gas ($CO_2/O_2/N_2$ mixture, 12.6/14/73,4% vol) is used as the feed gas. The water content in the feed gas is adjustable by using a water evaporator (IAS Model HOVACAL).

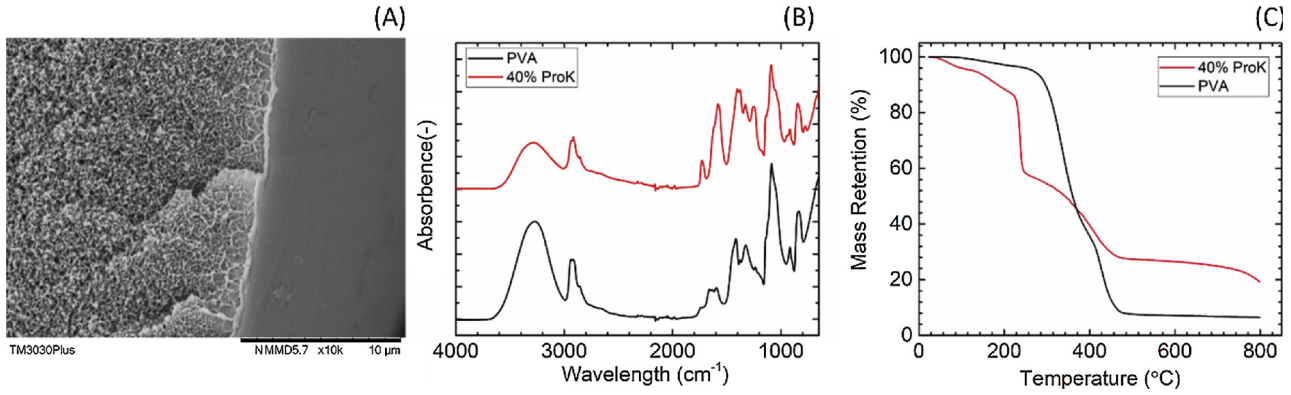


**Fig. 4.** Different characterization results for PVA/ProK-40 membranes, (A) SEM image, (B) FTIR and (C) TGA.

**Table 4**
. Permeance and selectivity of the PVA/ProK-40 membrane used at 20 °C.

| Membrane Batch | $CO_2$ permeance (GPU) | $\alpha_{CO2/N2}$ |
|---|---|---|
| 1 | 792.0 ± 5 | 40 |
| 2 | 799.5 ± 10 | 39 |

pressure in the permeate side is more stable, so the driving force across the membrane can be calculated with relatively small errors, which make it possible to report the $CO_2$ permeance with more reliable data. In the present study, $CO_2$ permeance of approximately 650 GPU was obtained, which is slightly lower than the values obtained from the lab scale test (~790 GPU). The different operation condition of the lab test (e.g., temperature, pressure, the presence of impurities in the feed stream) and the in-field test can be the main reasons for the deviation in these two values. In addition, the concentration polarization can also be an issue negatively affecting the separation performance.

Using sweep gas is usually considered not practical for post-combustion $CO_2$ capture as the permeate will then become a new mixture, thus extra energy is needed to separate the new mixture. However, Hao

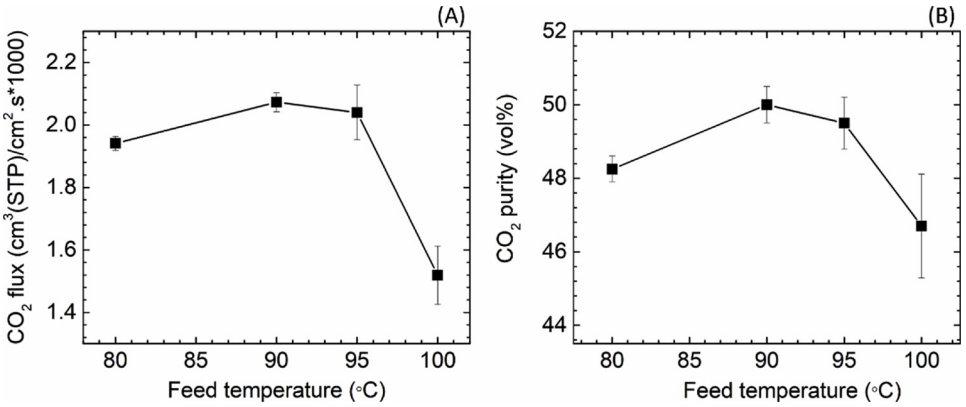


**Fig. 5.** Effect of temperature on membrane gas separation performances. Gas permeation tests were carried out with a feed pressure of 2 bar, feed flow rate 3.5 L/min with no sweep flow.

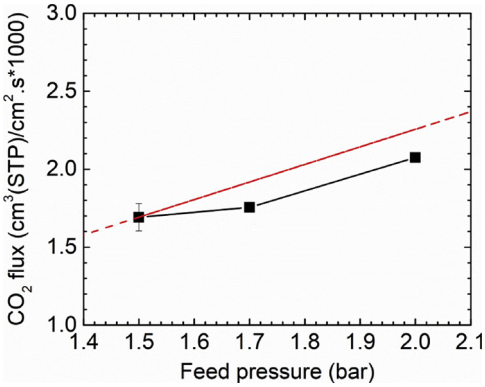


**Fig. 6.** Effect of feed pressure on membrane gas separation performances. Gas permeation tests were carried out with the feed pressure of 1.5 bar, temperature 90 °C, feed flow rate 3.5 L/min with no sweep flow.

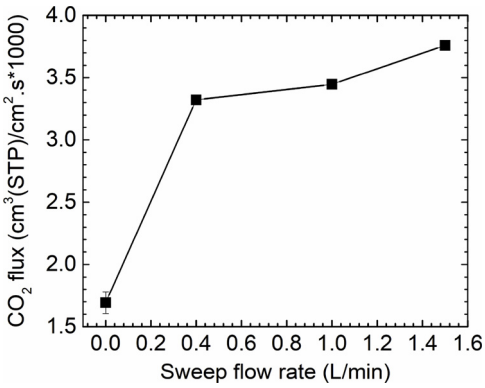


**Fig. 7.** Effect of sweep flow rate on membrane separation performances. Gas permeation tests were carried out with the feed pressure of 1.5 bar, temperature 90 °C, feed flow rate 3.5 L/min.

et al. reported a new process concept of using air as sweep gas flow in a post-combustion $CO_2$ capture process (Hao et al., 2014) where the permeate flow (air + $CO_2$) will be sent to the boiler. Although using this mixture slightly reduces the boiler efficiency, it significantly decreases the required membrane area for the separation. This concept was further studied in a pilot-scale test carried out in the National Carbon Capture Center in Wilsonville, Alabama, USA (White et al., 2015). Results reveal that a two-step membrane process combining vacuum and sweep gas can reach a 90% $CO_2$ capture efficiency.

In the current work, it is clearly shown that reducing the $CO_2$ partial pressure in the permeate side is more efficient than increasing the $CO_2$ partial pressure in the feed side (as shown in Fig. 7). Therefore, using sweep gas or vacuum on the permeate side can be a promising alternative design to increase the driving force and improve the membrane separation performances.

### 3.2.3. *Effect of vacuum grade*

A vacuum pump was added to the permeate stream to increase the gas transport driving force across the membrane. The use of vacuum in a membrane separation process for post-combustion $CO_2$ capture from a cement plant has previously been reported (Hägg et al., 2017; Sandru et al., 2013), in which the vacuum grade was controlled in the range of 0.2 bar–0.8 bar.

In the present study, similar to the case of using a sweep flow in the permeate side, an evident increase of $CO_2$ flux through the membrane can be observed when the vacuum was applied. From Fig. 8, it is clearly shown that the $CO_2$ flux first increased significantly with the vacuum grade (pressure from 1.0 bar to 0.4 bar), however, when the vacuum grade was too low (i.e., at 0.2 bar), there is a slight reduction in $CO_2$ flux. The possible reason can be that the high vacuum grade also removes the water from the membrane, reduced the membrane water uptake, thus reduced the amount of water which could contribute to the facilitated transport. Even though the driving force was slightly higher, the facilitated transport was hindered, leading to an overall reduction in the $CO_2$ flux across the membrane.

It is difficult to compare the separation performances obtained from different membranes and field tests due to the big differences in operational parameters (e.g., feed pressure, temperature, and vacuum grade). Even if the same membrane has been used, a doubled or even tripled $CO_2$ permeance or $CO_2/N_2$ selectivity may be obtained by

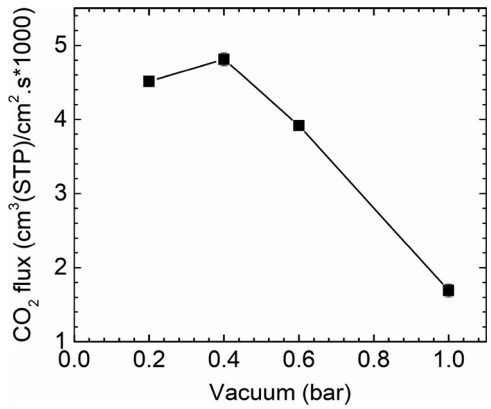


**Fig. 8.** Effect of vacuum grade on gas permeation through the membrane. Gas permeation tests were carried out with the feed pressure of 1.5 bar, temperature 90 °C, feed flow rate 3.5 L/min with no sweep flow.

changing operation parameters (Lin et al., 2014). Therefore, the separation performance results obtained in the current work was compared only to literature results obtained in similar conditions in terms of $CO_2$ flux. The unit of $CO_2$ flux was converted to $NLm^{-3}h^{-1}$ as reported in other literature for easier comparison. With a feed pressure of 1.5 bar and vacuum grade of 0.4 bar, a $CO_2$ flux of ~173 $NLm^{-3}h^{-1}$ was obtained from the current study. Compared to other reports carried out with similar feed pressure and vacuum grade (as shown in Table 1), this value is higher than that of the PVAm-based FSC membranes with the $CO_2$ flux of 20–80 $NLm^{-3}h^{-1}$ (He et al., 2017; Sandru et al., 2013). Facilitated transport membranes fabricated in Ho's group showed $CO_2$ permeance of ~800 GPU and $CO_2$ flux of ~160 $NLm^{-3}h^{-1}$, which is comparable with the tests in this study.

It should be aware that the pressure ratio, as well as the pressure on the feed side, should be taken into account in a gas separation process design (Huang et al., 2014). The combination of feed pressure and pressure ratio should be optimized from case to case.

### 3.2.4. Effect of water vapor in the feed gas

In facilitated transport membranes, it is well-known that the water content in the membrane is one of the key factors, which determines the $CO_2$ permeance and $CO_2/N_2$ selectivity. Therefore, in the current study, the water content in the feed side was changed to investigate the effect of the water on the separation performances. As the water content in the flue gas from the cement plant is fixed, synthetic flue gas $CO_2/O_2/N_2$ mixture (12.6/14/73.4% vol) from a gas cylinder was used to introduce water vapor. A water evaporator (IAS Model HOVACAL) was installed in the upstream of the membrane module to evaporate the desired amount of liquid water into water vapor before the synthetic flue gas was fed to the membrane module. The water content in the feed gas was adjusted from 8.7 to 20 vol%. The results of $CO_2$ flux across the membrane were shown in Fig. 9.

It is clearly seen that increasing the water content in the feed side could significantly improve the $CO_2$ flux in the membrane, especially from 8.7 to 10 vol%, demonstrating that the water vapor is dominating in the facilitated transport, and lower water content in the feed side resulted in a much lower $CO_2$ flux. Further increasing the water content in the feed gas only led to a moderate enhancement in the $CO_2$ flux, demonstrating that as long as the water vapor in the feed stream could fulfill the requirement of the facilitated transport, further increasing water content is less beneficial. In practical applications for facilitated transport membranes, a critical point of water content should be determined to reach the best separation performances as well as the most economical solution.

It has been reported for many facilitated transport membranes that impurities in the feed gas could significantly hinder the facilitated transport effect, even if at small quantities (Li et al., 2014). For instance, Wang and coworkers reported that the presence of 5000 ppm of SOx in the feed side resulted in a significant reduction (~20%) in $CO_2$ permeance for fixed carrier membranes (Li et al., 2014). Colin et al. reviewed the impact of different impurities on many polymeric membranes. They found that many minor components can affect performance both through competitive sorption and plasticization, while much remains unknown (Scholes et al., 2009). In addition, for facilitated transport membranes, oxidation of the facilitated transport agents is also another issue. If $O_2$ molecules present in the feed side under high temperature condition, the carriers (e.g., amine group) are more likely to be oxidized overtime and the membrane will gradually lose their facilitated transport abilities (Wang et al., 2013).

In the current study, there are many different impurities in the flue gas (e.g., NOx, CO, and $O_2$). As the synthetic gas only contains $CO_2$ and $N_2$, the impact of impurities on the membranes can also be observed in Fig. 9. The red dot is the separation result from real flue gas with the water content of 10.6 vol%. Compared to the result obtained from the synthetic gas with similar water content, the $CO_2$ flux from real flue gas is only slightly lower than the synthetic one, clearly shows that the impurities in the feed gas have a negligible (negative) effect on the separation performances.

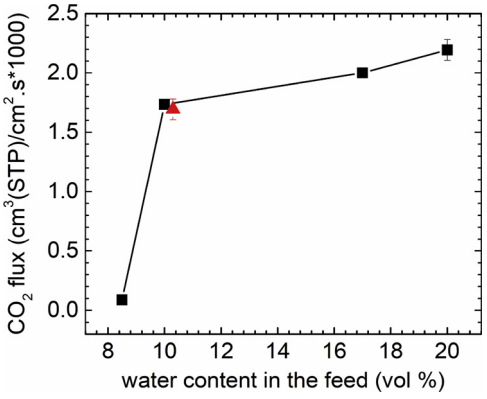


**Fig. 9.** Effect of water vapor content in the feed gas. Red dots represent the data from real flue gas with impurities. Gas permeation tests were carried out with the feed pressure of 1.5 bar, temperature 90 °C, feed flow rate 3.5 L/min with no sweep flow.

### 3.2.5. Stability test

Long-term stability is of critical importance for a membrane. It has been reported that almost all the commercially available gas separation membranes gradually lose half of their separation performance in the first few months (Baker and Low, 2014). For membranes based on solution-diffusion model, the loss of the gas permeance is mainly due to physical aging, such as the loss of free volume (by slow diffusing out of the membrane), which results in much lower permeance and slightly higher selectivity (Tiwari et al., 2014). In the case of facilitated transport membranes, the loss in membrane performances has been reported mainly due to irreversible reactions of impurities in the feed with the facilitated transport agents. The reactive impurities occupy the reaction sites of the carriers and reduce the facilitated transport efficiency (Li et al., 2014).

In the present study, the membrane showed stable separation performance in a one-day in-field test (as shown in Fig. 10) with only a slight increase for the $CO_2$ flux. However, when the test was carried out for 4 days and 6 days, the $CO_2$ flux reduced to only around half of the original value. The reduction of permeation performance over time in a real separation environment can be a function of a large number of variables, including physical/chemical aging, the suspended particulate matter size and loading, flue gas humidity, membrane hydrophobicity, and feed gas velocities. Facilitated transport membranes have proven to have good long-term stability at relatively low temperature conditions,

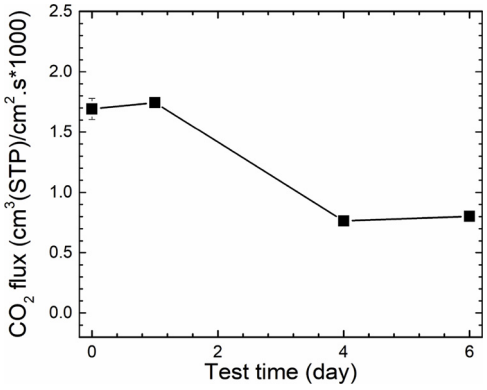


**Fig. 10.** Long-term stability performances, Gas permeation tests were carried out with the feed pressure of 1.5 bar, temperature 90 °C, feed flow rate 3.5 L/min with no sweep flow.

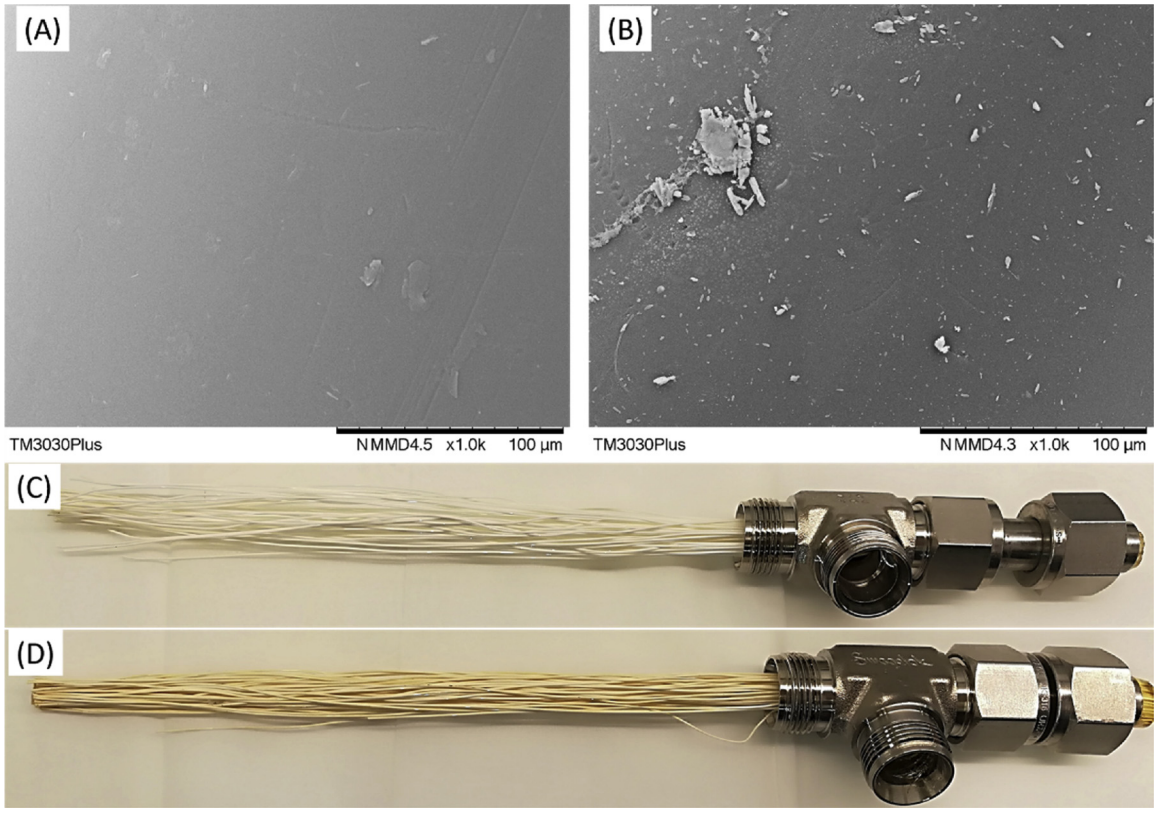


**Fig. 11.** Comparison of different chemical-physical properties of the hollow fiber membrane before and after the field test. SEM image of the membrane surface before (A) and after (B) field-test. Optical images of the hollow fiber before (C) and after (D) field test.

even with the presence of various impurities in the feed. For instance, facilitated transport membrane developed by Ho and co-workers exhibited a stable separation performance for approximately 700 h in a field test with a testing temperature of 57 °C (Han et al., 2019). In another study, the PVAm FSC membrane showed a stable $CO_2$ flux for over 500 h at ~40 °C (Hägg et al., 2017). Therefore, in the present study, the loss of the membrane performance is believed to be due to the oxidation of the reactive sites by the $O_2$ in the feed gas at the operating temperature. In addition, the occurrence of acidic water on the membranes may generate potential damage to the material.

In order to check the stability of the membrane, the membranes were characterized again after the field test and results are shown in Fig. 11.

As shown in Fig. 11, even though a 2-µm ceramic filter has been mounted in the sampling line before the flue gas being sent to the membrane module, there are still a significant number of particles on the membrane surface with the dimension from a few micrometer to tens of micrometers, some of which are bigger than the pore size of the filter. As the filter was found relative clean after the gas permeation test, the particles on the membrane surface are probably the smaller particles electrostatically adsorbed on the membrane surface and their aggregates. Alharthi et al. studied the effects of the flying ash on the membrane performance in post-combustion carbon capture applications (Alharthi et al., 2016). They found that flying ash has a less negative impact on the separation performances of the membrane. However, the negative impact becomes worse at humid conditions, and some of the impaction is irreversible, meaning that the membrane with "flying ash fouling" cannot be fully recovered. The "flying ash fouling" due to the effect of the suspended particulate matters is thus a possible explanation for the reduction in $CO_2$ flux in the long-term stability test as well.

The optical images of the membrane before and after the field tests were also recorded and presented in Fig. 11(C) and (D). A color change can be easily observed: the fresh membrane shows a white color, while after the field test, the membrane becomes brownish in color. The color change may be caused by the possible oxidation reaction that happened at high temperature conditions and/or due to the effect of the acidic components in the feed gas.

## 4. Conclusion

In the present study, pre-pilot scale PVA/amino acid salt hybrid hollow fiber membranes with a membrane area of around 200 $cm^2$ were produced at NTNU and tested at a cement plant. The effects of various operation parameters on gas separation performances have been systematically investigated. It is found that 90 °C is an optimized operation temperature in the investigated temperature range (80–115 °C) for the best separation performance. Compared to increasing the $CO_2$ partial pressure on the feed side, using a sweep flow or vacuum on the permeate side was found more effective in improving $CO_2$ flux across the membrane. The presence of various impurities in the feed stream only slightly reduced the $CO_2$ flux and $CO_2$ purity in the permeate side.

Stability of the facilitated transport membrane has also been studied for a duration of one week, and a reduction of $CO_2$ flux was recorded. The effect of the suspended particulate matter or the so-called "fly ash fouling", the oxidation of the facilitated transport agents under the relatively high temperature condition with the presence of $O_2$, and the effect of the acidic components in the feed stream may be the main causes of the reduced separation performance.

Further work may be done to optimize the operating temperature in order to achieve both high separation performances and good long-term stability. Meanwhile, the membrane and membrane module design may be further optimized to obtain the best operating conditions inside the modules and to reduce the concentration polarization effect for the separation.

The data obtained from this project provide a basis for the design

and fabrication of the pilot-scale hollow fiber module. Moreover, lessons learnt from the field test in this work reveal potential issues and give valuable experience, which would benefit the development of this membrane to a full pilot-scale test, moving the membrane technology and this membrane onto the next TRL (Technology Readiness Level) level.

## Conflicts of interest

There are no conflicts to declare.

## Acknowledgement

This work acknowledges the financial support from the European Union's Horizon 2020 Research and Innovation program under Grant Agreement No. 727734.

## References

Alharthi, K., Christianto, Y., Aguiar, A., Stickland, A., Stevens, G., Kentish, S., 2016. Impact of fly ash on the membrane performance in postcombustion carbon capture applications. Ind. Eng. Chem. Res. 55, 4711–4719. https://doi.org/10.1021/acs.iecr.6b00312.

Ansaloni, L., Zhao, Y., Jung, B.T., Ramasubramanian, K., Baschetti, M.G., Ho, W.S.W., 2015. Facilitated transport membranes containing amino-functionalized multi-walled carbon nanotubes for high-pressure $CO_2$ separations. J. Membr. Sci. 490, 18–28. https://doi.org/10.1016/j.memsci.2015.03.097.

Bai, H., Ho, W.S.W., 2009. New carbon dioxide-selective membranes based on sulfonated polybenzimidazole (SPBI) copolymer matrix for fuel cell applications. Ind. Eng. Chem. Res. 48, 2344–2354. https://doi.org/10.1021/ie800507r.

Bai, H., Ho, W.S.W., 2011. Carbon dioxide-selective membranes for high-pressure synthesis gas purification. Ind. Eng. Chem. Res. 50, 12152–12161. https://doi.org/10.1021/ie2007592.

Bains, P., Psarras, P., Wilcox, J., 2017. $CO_2$ capture from the industry sector. Prog. Energy Combust. Sci. 63, 146–172. https://doi.org/10.1016/j.pecs.2017.07.001.

Baker, R.W., Low, B.T., 2014. Gas separation membrane materials: a perspective. Macromolecules 47, 6999–7013. https://doi.org/10.1021/ma501488s.

Benson, S.M., Orr, F.M., 2008. Carbon dioxide capture and storage. MRS Bull. 33, 303–305. https://doi.org/10.1557/mrs2008.63.

Brinkmann, T., Naderipour, C., Pohlmann, J., Wind, J., Wolff, T., Esche, E., Müller, D., Wozny, G., Hoting, B., 2015. Pilot scale investigations of the removal of carbon dioxide from hydrocarbon gas streams using poly (ethylene oxide)–poly (butylene terephthalate) polyActive™) thin film composite membranes. J. Membr. Sci. 489, 237–247. https://doi.org/10.1016/j.memsci.2015.03.082.

Choi, S.-H., Kim, J.-H., Lee, Y., 2013. Pilot-scale multistage membrane process for the separation of $CO_2$ from LNG-fired flue gas. Sep. Purif. Technol. 110, 170–180. https://doi.org/10.1016/j.seppur.2013.03.016.

Dai, Z., Deng, J., Ansaloni, L., Janakiram, S., Deng, L., 2019. Thin-film-composite hollow fiber membranes containing amino acid salts as mobile carriers for $CO_2$ separation. J. Membr. Sci. 578 (15 May), 61–68. https://doi.org/10.1016/j.memsci.2019.02.023.

Deng, L., Hägg, M.-B., 2010. Swelling behavior and gas permeation performance of PVAm/PVA blend FSC membrane. J. Membr. Sci. 363, 295–301. https://doi.org/10.1016/j.memsci.2010.07.043.

Deng, L., Hägg, M.-B., 2014. Carbon nanotube reinforced PVAm/PVA blend FSC nanocomposite membrane for $CO_2/CH_4$ separation. Int. J. Greenhouse Gas Control 26, 127–134. https://doi.org/10.1016/j.ijggc.2014.04.018.

Deng, L., Hägg, M.-B., 2015. Fabrication and evaluation of a blend facilitated transport membrane for CO2/CH4 separation. Ind. Eng. Chem. Res. 54, 11139–11150. https://doi.org/10.1021/acs.iecr.5b02971.

Deng, L., Kim, T.-J., Hägg, M.-B., 2009. Facilitated transport of $CO_2$ in novel PVAm/PVA blend membrane. J. Membr. Sci. 340, 154–163. https://doi.org/10.1016/j.memsci.2009.05.019.

El-Azzami, L.A., Grulke, E.A., 2009. Carbon dioxide separation from hydrogen and nitrogen: facilitated transport in arginine salt-chitosan membranes. J. Membr. Sci. 328, 15–22. https://doi.org/10.1016/j.memsci.2008.08.038.

Galizia, M., Chi, W.S., Smith, Z.P., Merkel, T.C., Baker, R.W., Freeman, B.D., 2017. 50th anniversary perspective: polymers and mixed matrix membranes for gas and vapor separation: a review and prospective opportunities. Macromolecules 50, 7809–7843. https://doi.org/10.1021/acs.macromol.7b01718.

Hägg, M.-B., Lindbråthen, A., He, X., Nodeland, S., Cantero, T., 2017. Pilot demonstration-reporting on $CO_2$ capture from a cement plant using hollow fiber process. Energy Procedia 114, 6150–6165. https://doi.org/10.1016/j.egypro.2017.03.1752.

Han, Y., Salim, W., Chen, K.K., Wu, D., Ho, W.S.W., 2019. Field trial of spiral-wound facilitated transport membrane module for $CO_2$ capture from flue gas. J. Membr. Sci. 575, 242–251. https://doi.org/10.1016/j.memsci.2019.01.024.

Hao, P., Wijmans, J.G., Kniep, J., Baker, R.W., 2014. Gas/gas membrane contactors—an emerging membrane unit operation. J. Membr. Sci. 462, 131–138. https://doi.org/10.1016/j.memsci.2014.03.039.

He, X., Fu, C., Hägg, M.-B., 2015. Membrane system design and process feasibility analysis for $CO_2$ capture from flue gas with a fixed-site-carrier membrane. Chem. Eng. J. 268, 1–9. https://doi.org/10.1016/j.cej.2014.12.105.

He, X., Lindbråthen, A., Kim, T.-J., Hägg, M.-B., 2017. Pilot testing on fixed-site-carrier membranes for $CO_2$ capture from flue gas. Int. J. Greenhouse Gas Control 64, 323–332. https://doi.org/10.1016/j.ijggc.2017.08.007.

Huang, Y., Merkel, T.C., Baker, R.W., 2014. Pressure ratio and its impact on membrane gas separation processes. J. Membr. Sci. 463, 33–40. https://doi.org/10.1016/j.memsci.2014.03.016.

Kim, T.-J., Vrålstad, H., Sandru, M., Hägg, M.-B., 2013. Separation performance of PVAm composite membrane for $CO_2$ capture at various pH levels. J. Membr. Sci. 428, 218–224. https://doi.org/10.1016/j.memsci.2012.10.009.

Li, S., Wang, Z., He, W., Zhang, C., Wu, H., Wang, J., Wang, S., 2014. Effects of minor $SO_2$ on the transport properties of fixed carrier membranes for CO2 capture. Ind. Eng. Chem. Res. 53, 7758–7767. https://doi.org/10.1021/ie404063r.

Li, L., Wong-Ng, W., Huang, K., Cook, L.P., 2018. Materials and Processes for $CO_2$ Capture, Conversion, and Sequestration. John Wiley & Sons.

Lin, H., He, Z., Sun, Z., Vu, J., Ng, A., Mohammed, M., Kniep, J., Merkel, T.C., Wu, T., Lambrecht, R.C., 2014. $CO_2$-selective membranes for hydrogen production and $CO_2$ capture—part I: membrane development. J. Membr. Sci. 457, 149–161. https://doi.org/10.1016/j.memsci.2014.01.020.

Merkel, T.C., Lin, H., Wei, X., Baker, R., 2010. Power plant post-combustion carbon dioxide capture: an opportunity for membranes. J. Membr. Sci. 359, 126–139. https://doi.org/10.1016/j.memsci.2009.10.041.

Nunes, S.P., Peinemann, K.-V., 2006. Membrane Technology: in the Chemical Industry. John Wiley & Sons.

Pohlmann, J., Bram, M., Wilkner, K., Brinkmann, T., 2016. Pilot scale separation of $CO_2$ from power plant flue gases by membrane technology. Int. J. Greenhouse Gas Control 53, 56–64. https://doi.org/10.1016/j.ijggc.2016.07.033.

Qader, A., Webley, P.A., Stevens, G.W., Hooper, B., Harkin, T., Wiley, D.E., Kentish, S.E., Scholes, C.A., Smith, K., Mumford, K., Chen, V., 2017. Learnings from CO2CRC capture pilot plant testing—assessing technology development. Energy Procedia 114, 5855–5868. https://doi.org/10.1016/j.egypro.2017.03.1723.

Qin, Y., Lv, J., Fu, X., Guo, R., Li, X., Zhang, J., Wei, Z., 2016. High-performance SPEEK/amino acid salt membranes for $CO_2$ separation. RSC Adv. 6, 2252–2258. https://doi.org/10.1039/C5RA25089G.

Rafiq, S., Deng, L., Hägg, M.B., 2016. Role of facilitated transport membranes and composite membranes for efficient CO2 capture—a review. ChemBioEng Rev. 3, 68–85. https://doi.org/10.1002/cben.201500013.

Salim, W., Vakharia, V., Chen, Y., Wu, D., Han, Y., Ho, W.S.W., 2018. Fabrication and field testing of spiral-wound membrane modules for $CO_2$ capture from flue gas. J. Membr. Sci. 556, 126–137. https://doi.org/10.1016/j.memsci.2018.04.001.

Sandru, M., Kim, T.-J., Capala, W., Huijbers, M., Hägg, M.-B., 2013. Pilot scale testing of polymeric membranes for $CO_2$ capture from coal fired power plants. Energy Procedia 37, 6473–6480. https://doi.org/10.1016/j.egypro.2013.06.577.

Scholes, C.A., Kentish, S.E., Stevens, G.W., 2009. Effects of minor components in carbon dioxide capture using polymeric gas separation membranes. Sep. Purif. Rev. 38, 1–44. https://doi.org/10.1080/15422110802411442.

Scholes, C.A., Qader, A., Stevens, G.W., Kentish, S.E., 2015. Membrane pilot plant trials of $CO_2$ separation from flue gas. Greenhouse Gases: Sci. Technol. 5, 229–237. https://doi.org/10.1002/ghg.1498.

Tiwari, R.R., Smith, Z.P., Lin, H., Freeman, B.D., Paul, D.R., 2014. Gas permeation in thin films of "high free-volume" glassy perfluoropolymers: part I. Physical aging. Polymer 55, 5788–5800. https://doi.org/10.1016/j.polymer.2014.09.022.

Tong, Z., Ho, W.W., 2017. Facilitated transport membranes for $CO_2$ separation and capture. Sep. Sci. Technol. 52, 156–167. https://doi.org/10.1080/01496395.2016.1217885.

Wang, M., Wang, Z., Li, S., Zhang, C., Wang, J., Wang, S., 2013. A high performance antioxidative and acid resistant membrane prepared by interfacial polymerization for $CO_2$ separation from flue gas. Energy Environ. Sci. 6, 539–551. https://doi.org/10.1039/C2EE23080A.

Ward, W.J., Robb, W.L., 1967. Carbon dioxide-oxygen separation: facilitated transport of carbon dioxide across a liquid film. Science 156, 1481–1484. https://doi.org/10.1126/science.156.3781.1481.

Way, J.D., Noble, R.D., 1992. Facilitated transport. In: Ho, W.S.W., Sirkar, K.K. (Eds.), Membrane Handbook. Springer, Boston, MA, US, pp. 833–866.

Way, J., Noble, R., Reed, D., Ginley, G., Jarr, L., 1987. Facilitated transport of $CO_2$ in ion exchange membranes. AlChE J. 33, 480–487.

White, L.S., Wei, X., Pande, S., Wu, T., Merkel, T.C., 2015. Extended flue gas trials with a membrane-based pilot plant at a one-ton-per-day carbon capture rate. J. Membr. Sci. 496, 48–57. https://doi.org/10.1016/j.memsci.2015.08.003.

Wolff, T., Brinkmann, T., Kerner, M., Hindersin, S., 2015. $CO_2$ enrichment from flue gas for the cultivation of algae—a field test. Greenhouse Gases: Sci. Technol. 5, 505–512.

Xing, R., Ho, W.S.W., 2011. Crosslinked polyvinylalcohol–polysiloxane/fumed silica mixed matrix membranes containing amines for $CO_2/H_2$ separation. J. Membr. Sci. 367, 91–102. https://doi.org/10.1016/j.memsci.2010.10.039.

Yave, W., Car, A., Funari, S.S., Nunes, S.P., Peinemann, K.-V., 2010. $CO_2$-philic polymer membrane with extremely high separation performance. Macromolecules 43, 326–333. https://doi.org/10.1021/ma901950u.

Yegani, R., Hirozawa, H., Teramoto, M., Himei, H., Okada, O., Takigawa, T., Ohmura, N., Matsumiya, N., Matsuyama, H., 2007. Selective separation of $CO_2$ by using novel facilitated transport membrane at elevated temperatures and pressures. J. Membr. Sci. 291, 157–164. https://doi.org/10.1016/j.memsci.2007.01.011.